A High-Throughput RNA Displacement Assay for Screening SARS-CoV-2 nsp10-nsp16 Complex toward Developing Therapeutics for COVID-19

Sumera Perveen[1], Aliakbar Khalili Yazdi[1], Kanchan Devkota[1], Fengling Li[1], Pegah Ghiabi[1], Taraneh Hajian[1], Peter Loppnau[1], Albina Bolotokova[1], and Masoud Vedadi[1,2] (iD)

Abstract

SARS-CoV-2, the coronavirus that causes COVID-19, evades the human immune system by capping its RNA. This process protects the viral RNA and is essential for its replication. Multiple viral proteins are involved in this RNA capping process, including the nonstructural protein 16 (nsp16), which is an *S*-adenosyl-ʟ-methionine (SAM)-dependent 2′-*O*-methyltransferase. Nsp16 is significantly active when in complex with another nonstructural protein, nsp10, which plays a key role in its stability and activity. Here we report the development of a fluorescence polarization (FP)-based RNA displacement assay for nsp10-nsp16 complex in a 384-well format with a Z′ factor of 0.6, suitable for high-throughput screening. In this process, we purified the nsp10-nsp16 complex to higher than 95% purity and confirmed its binding to the methyl donor SAM, the product of the reaction, *S*-adenosyl-ʟ-homocysteine (SAH), and a common methyltransferase inhibitor, sinefungin, using isothermal titration calorimetry (ITC). The assay was further validated by screening a library of 1124 drug-like compounds. This assay provides a cost-effective high-throughput method for screening the nsp10-nsp16 complex for RNA competitive inhibitors toward developing COVID-19 therapeutics.

Introduction

Over the last two decades, major outbreaks of coronaviruses have been endured worldwide. These include zoonotic epidemics of severe acute respiratory syndrome coronavirus (SARS-CoV) in 2002,[1] Middle East respiratory syndrome coronavirus (MERS-CoV) in 2012,[2,3] and the current pandemic of SARS-CoV-2 that started in 2019 (COVID-19).[4] With more than 56 million confirmed COVID-19 infections and more than 1.3 million deaths so far (November 20, 2020; World Health Organization; https://www.who.int/emergencies/diseases/novel-coronavirus-2019), the COVID-19 pandemic has had widespread global socioeconomic implications and overwhelmed healthcare systems worldwide.

Coronavirus is a member of the subfamily Coronavirinae within the family Coronaviridae.[5,6] Many species can be infected by CoVs.[6] However, only seven coronaviruses have been documented to infect humans to date.[4,7] These include SARS-CoV, MERS-CoV, and SARS-CoV-2 which could cause severe symptoms leading to higher fatalities.[4]

Infection of 229E, HKU1, OC43, and NL63 has been associated with a range of relatively mild respiratory diseases.[7] SARS-CoV-2 shares 79.6% RNA sequence identity with SARS-CoV.[8] Coronaviruses are enveloped, nonsegmented positive-sense RNA viruses that have the largest genome among RNA viruses.[9,10] They encode 16 nonstructural proteins (nsps) that play essential roles in RNA replication and

[1]Structural Genomics Consortium, University of Toronto, Toronto, ON, Canada
[2]Department of Pharmacology and Toxicology, University of Toronto, Toronto, ON, Canada

Corresponding Author:
Masoud Vedadi, Structural Genomics Consortium, University of Toronto, 101 College St. 7 Floor, Room 714, Toronto, ON M5G 1L7, Canada.
Email: m.vedadi@utoronto.ca

processing of subgenomic RNA.[8,11–13] SARS-CoV-2 replication involves RNA synthesis, proofreading, and capping.[14] Coronavirus mRNAs are protected at their 5′ ends by a cap structure consisting of an N7-methylated guanine linked to the first transcribed nucleotide by a 5′-5′ triphosphate bond and 2′-*O*-methylation (N7-meGpppN-2′-*O*-me) (**Suppl. Fig. S1**).[15] The RNA capping is essential for the stability of viral mRNA and evading the host immune system. Uncapped RNA molecules are identified as "foreign" by a host's innate immune response and undergo degradation.[16,17] Therefore, proteins catalyzing RNA capping are attractive targets for antiviral drug development. Nsps involved in viral mRNA capping include nsp10 (cofactor for nsp14 and nsp16),[18] nsp13 (RNA 5′-triphosphatase, helicase),[19] nsp14 (guanine-N7 methyltransferase),[20] and nsp16 (2′-*O*-methyltransferase).[17,21,22]

The capping process begins with the removal of the 5′γ-phosphate of the newly synthesized RNA chains (pppN-RNA) by nsp13.[19] Then a guanylyltransferase (GTase) catalyzes the formation of GpppN-RNA by transferring a guanosine monophosphate (GMP) molecule to the 5′-diphosphate of the RNA chains (ppN-RNA). Nsp14 methylates the cap structure at the N7 position of the guanosine, resulting in the formation of cap-0 (N7-meGpppN-RNA).[20] Ultimately, the nsp10-nsp16 complex catalyzes the addition of a methyl group on the ribose 2′-*O* position of the first transcribed nucleotide of the cap-0 to form a cap-1 (N7-meGpppNme-RNA) (**Suppl. Fig. S1**).[22,23] In vitro, methyltransferase activity has been reported for nsp10-nsp16 complexes from feline coronavirus (FCoV),[24] SARS-CoV,[22] and MERS-CoV,[25] and the binding of various RNAs to MERS-CoV has been assessed and used to rank-order substrates.[25] Nsp10 acts as an allosteric activator of nsp16 and is essential for its stability and activity,[17,26] increasing its binding affinity for RNA substrate and SAM in both SARS-CoV and MERS-CoV.[17] Various structures of nsp10-nsp16 from SARS-CoV-2 in complex with SAM, SAH, RNA, and sinefungin have been recently deposited in the Protein Data Bank (PDB) that provide vast amounts of information on the interaction of substrates with nsp16 and could be used in structure-guided drug discovery.[27,28]

One of the cost-effective ways of screening for RNA substrate competitive inhibitors is to label the RNA with fluorescein and detect its binding to the target RNA methyltransferase by monitoring the change in fluorescent polarization signal.[29] Here we report the development of a fluorescence polarization (FP)-based RNA displacement assay that is suitable for high-throughput screening of the nsp10-nsp16 complex against large libraries of compounds to identify RNA competitive inhibitors of nsp16 methyltransferase activity. This assay is also a perfect tool for triaging a high number of potential inhibitors from screening by alternative methods for competing with RNA substrate and determining their mechanism of inhibition.

Materials and Methods

Reagents

S-adenosyl-L-methionine (SAM), *S*-adenosyl-L-homocysteine (SAH), and sinefungin were purchased from Sigma-Aldrich (Oakville, Canada). Fluorescein amidite (FAM)-labeled RNA (5′ N7-meGpppACCCCC-FAM 3′) and biotinylated RNA (5′ N7-meGpppACCCCC-Biotin 3′) were purchased from bioSYNTHESIS (Levisville, TX). The unlabeled Cap RNA, m7G(5′)ppp(5′G (NEB, cat. S1404S) and m7G(5′)ppp(5′)A (NEB, cat. S1405S), also referred to as N7-meGpppG and N7-meGpppA for consistency, respectively; G(5′)ppp(5′)A RNA (GpppA) (NEB, cat. S1406S); and G(5′)ppp(5′)G RNA (GpppG) (NEB, cat. S1407S) are from New England Biolabs (NEB, Whitby, Ontario, Canada). NEB RNA reagents were gifts from Dr. Peter Stogios, University of Toronto. All RNA solutions were prepared by dissolving in nuclease-free water, in the presence of RNAseOUT (Life Technologies Calstad, CA) at a final concentration of 0.4 U/μL.

Protein Purification

His-tagged nsp10 (residues A1–Q139) and nsp16 (S1–N298) were expressed in *Escherichia coli* separately and purified to homogeneity using Ni-NTA resin. Purified nsp10 and nsp16 proteins were mixed at a molar ratio of 8 to 1, respectively, to prepare a stable and functional complex. The expression and purification of nsp10 and nsp16, and nsp10-nsp16 complex preparation are described in detail in the supplemental data (**Suppl. Figs. S2–S4**).

FP-Based RNA Displacement Assays

All FP experiments were performed in a total assay volume of 20 μL per well in 384-well black polypropylene PCR plates (PCR-384-BK, Axygen, Tewksbury, MA) using FAM-labeled RNA (5′ N7-meGpppACCCCC-FAM 3′) and the nsp10-nsp16 complex. FP was measured after 30 min of incubation at room temperature, using a BioTek Synergy 4 (BioTek, Winooski, VT) with excitation and emission wavelengths of 485 nm and 528 nm, respectively. All experiments were performed in triplicate (n = 3), and plotted values are the average of three replicates ± standard deviation. The FP values were blank subtracted and were presented as the percentage of control (FP %). Data were visualized using GraphPad Prism software 7.04 (GraphPad, La Jolla, CA).

For assessing the binding of FAM-RNA (5′ N7-meGpppACCCCC-FAM 3′) to the nsp10-nsp16 complex, varying concentrations of the protein were incubated with 30 nM FAM-RNA in 10 mM Tris(hydroxymethyl)aminomethane (Tris) buffer, pH 7.5, containing 5 mM DTT, 0.01% Triton X-100, and 0.01% bovine serum albumin (BSA) for 30 min at room temperature in 20 μL of reaction volume. FP (485 nm/528 nm) was measured using a Biotek

Synergy H1. The change in FP (mP) was plotted as a function of the nsp10-nsp16 concentration. The concentration of protein corresponding to the half-maximum FP signal (K_d) and the maximum FP signal (Bmax) was calculated using nonlinear least-squares regression to a single-site binding model in GraphPad Prism 7.04.[29]

To establish the specificity of the assay, a mixture containing 0.5 µM nsp10-nsp16 complex and 30 nM FAM-RNA, in 10 mM Tris buffer, pH 7.5, containing 5 mM DTT, 0.01% Triton X-100, and 0.01% BSA, was incubated separately with varying concentrations of unlabeled RNA cap analogs: N7-meGpppG, N7-meGpppA, GpppG, and GpppA in 20 µL reaction volumes for 30 min at room temperature. The FP values were determined, and the K_{disp} (K displacement) values (the concentrations required for 50% displacement of the labeled RNA) were calculated using nonlinear least-squares regression analysis to a four-parameter concentration–response curve model in GraphPad Prism 7.04.

Z'-Factor Determination

The Z' factor was determined by incubating the nsp10-nsp16 complex (0.5 µM) with 30 nM FAM-RNA in the presence or absence of 50 µM unlabeled RNA (N7-meGpppA) in a 384-well plate for 30 min at room temperature (168 wells each). FP was measured as described above.

Screening Compounds from the Prestwick Library

The Prestwick Chemical Library was purchased from Prestwick Chemicals and screened using optimized assay conditions (10 mM Tris buffer, pH 7.5, containing 5 mM DTT, 0.01% Triton X-100, and 0.01% BSA) at a 50 µM compound concentration, with 0.5% DMSO concentration in 384-well black polypropylene PCR plates (Axygen, Tewksbury, MA, cat. PCR-384-BK) with a final reaction volume of 20 µL for 30 min at room temperature. Data were analyzed using GraphPad Prism 7.04 as described above.

Isothermal Titration Calorimetry

Binding of SAM, SAH, and sinefungin to the nsp10-nsp16 (8:1) complex was tested by Nano isothermal titration calorimetry (ITC; TA Instruments–Waters LLC, New Castle, DE) at 25 °C. The nsp10-nsp16 complex was dialyzed against 50 mM Tris-HCl buffer, pH 8.0, containing 200 mM NaCl and was loaded into the sample cell (300 µL) at a concentration of 48 µM, and a solution of 500 µM ligand (SAM, SAH, or sinefungin) was placed in the injection syringe (50 µL). Data were fitted with a one-binding-site model using TA Instruments origin software.

Results and Discussion

SARS-COV-2 nsp10-nsp16 Complex Preparation and Quality Control

The nsp10-nsp16 complex was prepared in an 8 (nsp10) to 1 (nsp16) ratio (**Suppl. Fig. S2**). The complex formation was evaluated and confirmed by size exclusion chromatography (**Suppl. Fig. S3**). In addition, the presence of nsp10 and nsp16 in the complex fractions was verified by mass spectrometry (**Suppl. Fig. S4**). To evaluate the functional integrity of the prepared complex, the binding of the methyl donor SAM, the product of the reaction SAH, and a common methyltransferase inhibitor sinefungin were tested using ITC. The nsp10-nsp16 complex showed binding to SAM, SAH, and sinefungin with K_d values of 3.4 ± 1.5 µM, 5.7 ± 1.9 µM, and 6.8 ± 2.0 µM, respectively, indicating that the protein complex was formed and maintained the expected active site conformation (**Fig. 1**). SAM has been previously reported to promote active MERS nsp10-nsp16 complex assembly.[25] The K_d values reported for SAM binding to the SARS-CoV nsp10-nsp16 complex (K_d = 5.59 ± 1.15 µM)[21] are within the same range as we report for SARS-CoV-2 nsp10-nsp16 complex binding to SAM (K_d = 3.4 ± 1.5 µM). This indicates the highly conserved interaction of co-factor SAM with the nsp10-nsp16 complex from these coronaviruses.

RNA Displacement Assay Development

The FAM-labeled RNA was used to set up the RNA displacement assay. Binding of this RNA to the nsp10-nsp16 complex was confirmed by detecting a significant increase in FP signal (**Suppl. Fig. S5**). Various buffer conditions such as 4-(2-hydroxyethyl)-1-piperazineethanesulfonic acid (HEPES), Bis-Tris propane (BTP), sodium phosphate (NaP), Tris, and potassium phosphate (KP) at 20 mM, pH 7.5, were tested and the FP signal was relatively higher in Tris and HEPES than other buffers (**Suppl. Fig. S5A**). Tris at 10 mM provided the highest signal and was selected for testing additives (**Suppl. Fig. S5B**). The signal was unaffected up to 1% BSA, 10 mM TCEP, KCl, and $MgCl_2$ (**Suppl. Fig. S5C–F**). The pH profile showed pH 7.5 as optimum (**Fig. 2A**). The signal was not significantly affected by increasing concentrations of DTT (**Fig. 2B**) and NaCl (**Fig. 2C**) or EDTA (**Fig. 2D**) up to 10 mM. Triton X-100 (**Fig. 2E**) and DMSO (**Fig. 2F**) had no significant effect on signal up to 1% and 5%, respectively. DTT was selected to be used at 5 mM in assays to maintain a reducing environment. The addition of Triton X-100 at 0.01% is expected to help minimize the binding of fluorophores and proteins to polystyrene plates and compound aggregate formation during screening.[30,31] BSA was also included at 0.01% to prevent nonspecific interactions. Based on optimization results, the
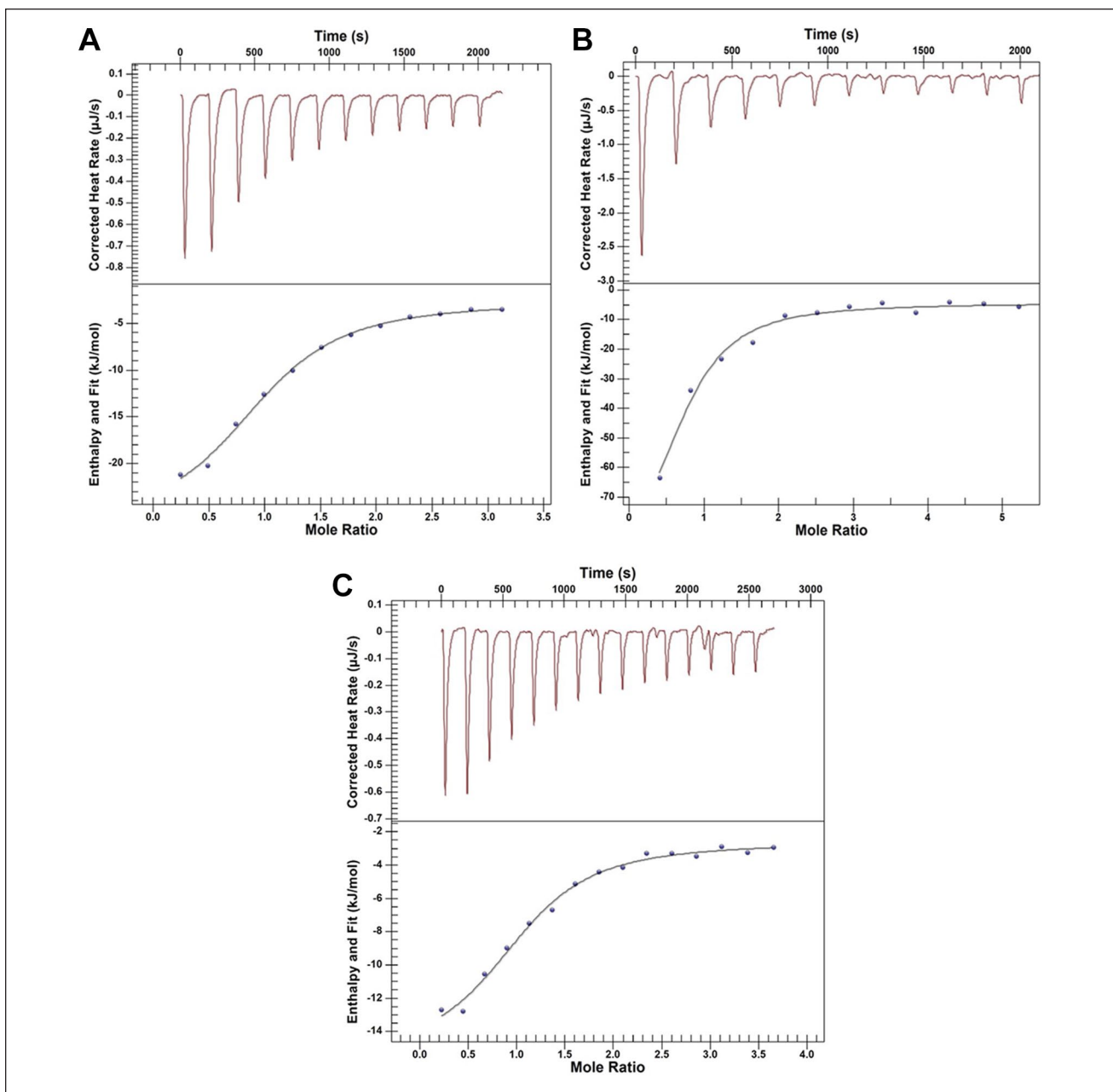
Figure 1. Binding assay. Binding of the nsp10-nsp16 complex to (**A**) SAM, (**B**) SAH, and (**C**) sinefungin was confirmed by ITC with K_d values of 3.4 $\pm$ 1.5 μM, 5.7 $\pm$ 1.9 μM, and 6.8 $\pm$ 2.0 μM, respectively. The K_d values are the mean $\pm$ standard deviation from three independent experiments.

final assay conditions consist of 5 mM DTT, 0.01% Triton X-100, and 0.01% BSA in 10 mM Tris buffer, pH 7.5, and an incubation time of 30 min.

Using the optimized assay conditions, the nsp10-nsp16 complex showed concentration-dependent binding to the FAM-RNA at 30 nM with an apparent K_d of 0.13 $\pm$ 0.002 μM and *B*max of 270 $\pm$ 5 mP (**Table 1, Fig. 3A**). For RNA displacement assays, the protein complex concentration

was kept at 80% of the maximum signal (0.5 μM) to allow better competitive displacement. Unlabeled methylated RNA cap analogs N7-meGpppG and N7-meGpppA were used to compete off the FAM-RNA binding to the nsp10-nsp16 complex. Both N7-meGpppG and N7-meGpppA displaced FAM-RNA with K_{disp} values of 17 $\pm$ 3 μM and 20 $\pm$ 6 μM, respectively (**Table 1, Fig. 3B,C**), while unlabeled unmethylated cap analogs GpppG (**Fig. 3D**) and GpppA
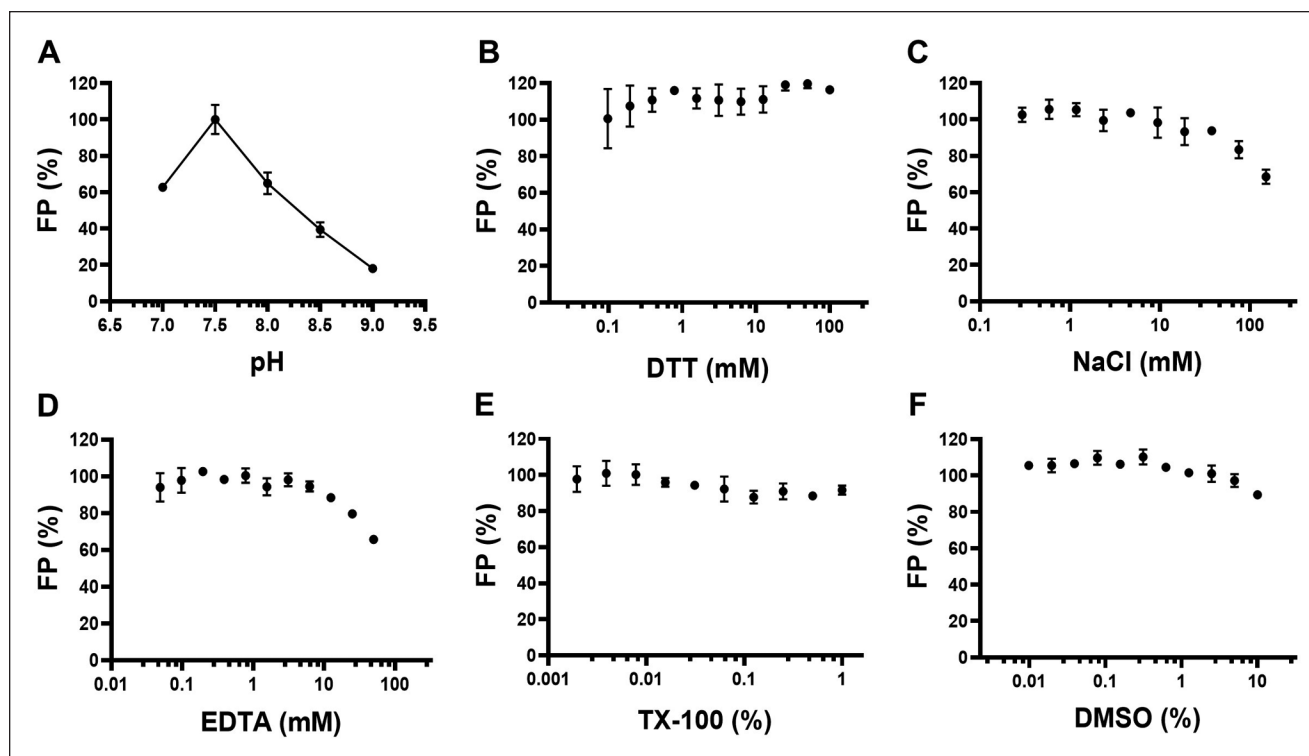
Figure 2. FP assay optimization for nsp10-nsp16 interaction with N7-meGpppACCCCC-FAM. The FP signal from the interaction of 0.5 μM nsp10-nsp16 complex with 30 nM N7-meGpppACCCCC-FAM was evaluated at (**A**) a pH range of 7.0 to 9.0 in 10 mM Tris buffer. The effect of additives such as (**B**) DTT, (**C**) NaCl, (**D**) EDTA, (**E**) Triton X-100, and (**F**) DMSO was evaluated in 10 mM Tris, pH 7.5. Plotted values are the mean ± standard deviation of three independent experiments. The FP values are blank subtracted and presented as a percentage of the control. In **A**, pH 7.5 was considered as 100% signal. Data were analyzed using GraphPad Prism software 7.0.4.

Table 1. RNA Displacement.

RNA	K_d (μM)	K_{disp} (μM)
N7-me GpppACCCCC-FAM	0.13 ± 0.002	NA
N7-me GpppG	NA	17 ± 3
N7-me GpppA	NA	20 ± 6
GpppG	NA	No displacement
GpppA	NA	No displacement

All values are from **Figure 3.**
NA, not applicable; K_{disp}, K displacement.[29]

(**Fig. 3E**) were unable to displace FAM-RNA from the nsp10-nsp16 complex. C-terminally biotinylated 5′ N7-methylated GpppACCCCC 3′ also displaced the FAM-RNA with a K_{disp} of 4.3 μM (**Suppl. Fig. S6**). These observations further confirmed that the nsp10-nsp16 protein complex specifically recognizes its N7-me RNA substrate.

To determine whether the RNA displacement assay at optimized conditions is amenable to high-throughput screening, the Z′ factor was determined by performing the assay in a 384-well format using FAM-RNA (5′ N7-meGpppACCCCC-FAM 3′) in the presence (168 data points) and absence (168 data points) of 50 μM unlabeled RNA (N7-meGpppA). The calculated Z′ factor was 0.6, indicating that the assay is suitable for screening for RNA competitive inhibitors (**Fig. 3F**).

The FAM-labeled RNA substrate in this study was designed based on the previous studies on the SARS-CoV nsp10-nsp16 complex reporting recognition of cap-0 RNA as substrate but not N7-meGpppG-capped RNA.[21] In vitro, RNA substrate for SARS-CoV nsp10-nsp16 needs to be N7-guanine methylated with adenine as the first nucleotide.[22] Similarly, no RNA displacement with the SARS-CoV-2
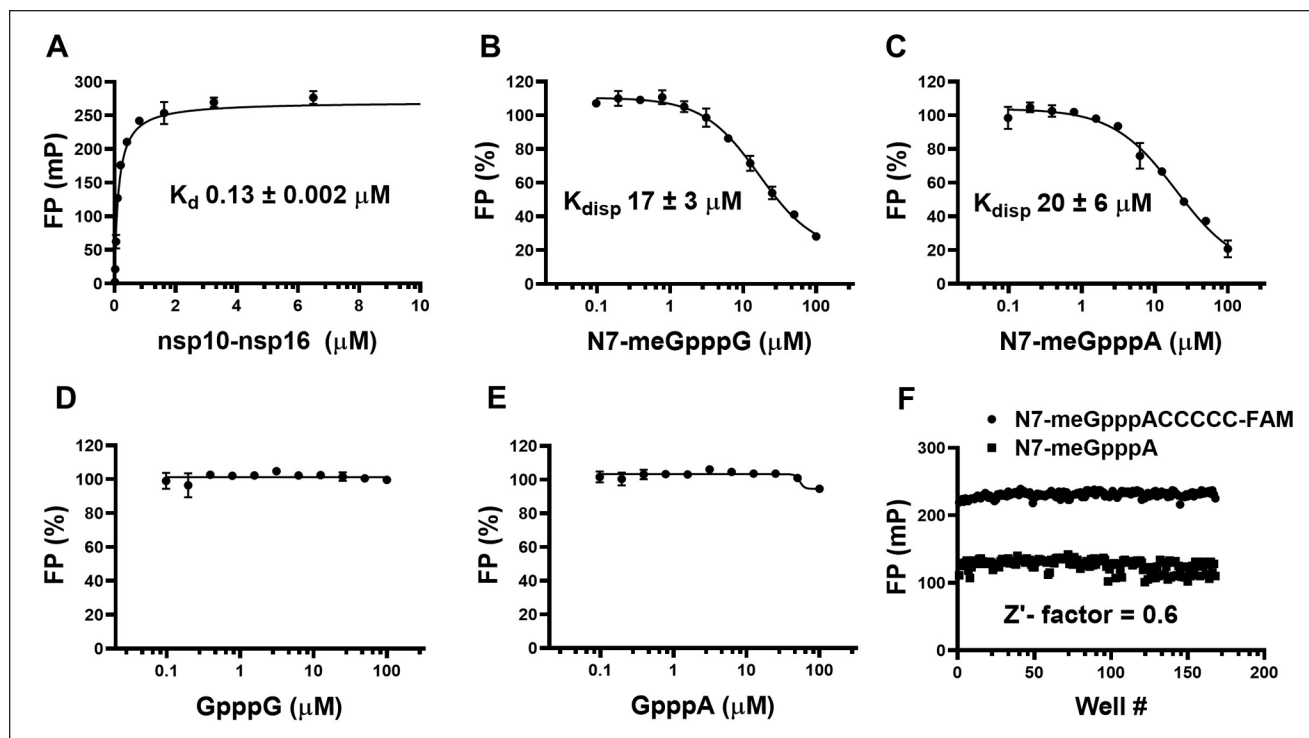
Figure 3. FP saturation binding and competitive displacement curves for the nsp10-nsp16 complex. (**A**) The nsp10-nsp16 complex binds to 5′ N7-meGpppACCCCC-FAM 3′ with a K_d of 0.13 ± 0.002 μM and *B*max of 270 ± 5 mP. Unlabeled methylated cap RNAs, (**B**) N7-meGpppG and (**C**) N7-meGpppA, compete with 5′ N7-meGpppACCCCC-FAM 3′ for binding to the nsp10-nsp16 complex. Unlabeled unmethylated cap RNAs, (**D**) GpppG and (**E**) GpppA, did not disrupt the interaction between the nsp10-nsp16 complex and RNA-FAM. All values are the mean ± standard deviation of three independent experiments. (**F**) The Z′ factor (0.6) was determined for evaluation of the assay for high-throughput screening. FAM-labeled RNA (5′ N7-meGpppACCCCC-FAM 3′) at 30 nM was used to generate the FP signal, while 50 μM unlabeled RNA (N7-meGpppA) was used as a positive control. Data were analyzed using GraphPad Prism software 7.0.4.

nsp10-nsp16 complex using the unmethylated RNA samples, such as GpppA and GpppG, was observed. These observations are also consistent with reports on similar binding assays with SARS-CoV[17] and MERS-CoV[25] proteins, where nsp16 can discriminate the cap-0 (N7-meGpppN-RNA) from an unmethylated RNA (GpppN-RNA).

Screening a Library of 1124 Compounds

A collection of 1124 drugs and drug-like compounds was screened. Initially, 15 compounds were identified as potential antagonists of nsp10-nsp16-RNA interaction based on reduction of polarization signal (>50% reduction) compared with the control at a 50 μM final compound concentration (**Fig. 4**).

All 15 compounds were tested for any possible interference with the signal readout, and 12 compounds showed a significant effect and were eliminated. Three compounds showed dose-dependent displacement with no signal interference. However, considering the high Hill slopes as a red flag, we further tested the binding of these three compounds

to the nsp10-nsp16 complex by ITC, and none of the compounds were confirmed. This screening exercise confirmed the suitability of the optimized RNA displacement assay for medium- to high-throughput screening of the nsp10-nsp16 complex with a low number of false positives.

Limitation of the Assay

Methyltransferases have been shown to be druggable,[32] with more than 20 potent, selective, and cell-active small molecules (chemical probes) discovered for such enzymes in the last decade.[32] Typically, both SAM[33] and substrate binding sites of methyltransferases can be targeted for drug discovery.[32] The optimized FP-based RNA displacement assay for the nsp10-nsp16 complex is suitable for high-throughput screening to identify RNA competitive inhibitors. This assay is also suitable for triaging RNA competitive small molecules from a high number of hits identified by other methods. However, the RNA displacement assay will not detect SAM competitive inhibitors, unless they partially affect RNA binding. In addition, compounds that affect the
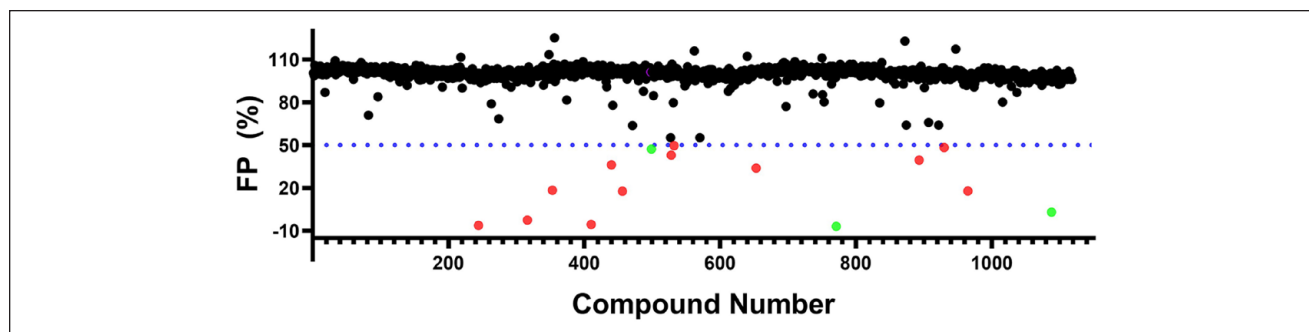
Figure 4. Screening Prestwick Compound Library. The distribution of the readout for 1124 compounds screened by the RNA displacement assay is shown. Compounds that significantly reduced the polarization signal (>50%) compared with the control were selected as screening hits (highlighted in red). Three compounds (highlighted in green) showed concentration-dependent inhibition. However, none of these compounds showed any binding when tested by ITC (data not shown).

FP signal or interact with RNA substrate could potentially increase the number of false positives. It is critical to confirm the RNA displacement-based screening hits by activity-based assays, and orthogonal methods such as ITC before the start of follow-up chemistry.

Conclusion

The COVID-19 pandemic has an unprecedented impact on the global economy and has already brought the healthcare services worldwide to a breaking point. So far, there is no effective drugs for this disease. Even vaccines developed today may not be effective on future mutated variants.[34] This necessitates the development of therapeutics that could stop the replication of the SARS-CoV-2. The RNA displacement assay in a 384-well format presented in this study provides a cost-effective method to screen the nsp10-nsp16 complex against large libraries of compounds to identify small-molecule RNA competitive inhibitors. Such molecules could lead to developing therapeutics for COVID-19 through inhibition of viral replication, and likely would be effective on other coronaviruses due to the high sequence conservation of nsp16 among this family of viruses.

ORCID iD

Masoud Vedadi 🆔 https://orcid.org/0000-0002-0574-0169

References

1. Chan-Yeung, M.; Xu, R. H. SARS: Epidemiology. *Respirology* **2003**, *8* (Suppl.), S9–S14.
2. Yao, T. T.; Qian, J. D.; Zhu, W. Y.; et al. A Systematic Review of Lopinavir Therapy for SARS Coronavirus and MERS Coronavirus—A Possible Reference for Coronavirus Disease-19 Treatment Option. *J. Med. Virol.* **2020**, *92*, 556–563.
3. Zaki, A. M.; Van Boheemen, S.; Bestebroer, T. M.; et al. Isolation of a Novel Coronavirus from a Man with Pneumonia in Saudi Arabia. *N. Engl. J. Med.* **2012**, *367*, 1814–1820.
4. Andersen, K. G.; Rambaut, A.; Lipkin, W. I.; et al. The Proximal Origin of SARS-CoV-2. *Nat. Med.* **2020**, *26*, 450–452.
5. Adams, M. J.; Carstens, E. B. Ratification Vote on Taxonomic Proposals to the International Committee on Taxonomy of Viruses. *Arch. Virol.* **2012**, *157*, 1411–1422.
6. Coronaviridae Study Group of the International Committee on Taxonomy of Viruses. The Species Severe Acute Respiratory Syndrome-Related Coronavirus: Classifying 2019-nCoV and Naming It SARS-CoV-2. *Nat. Microbiol.* **2020**, *5*, 536–544.
7. Corman, V. M.; Muth, D.; Niemeyer, D.; et al. Hosts and Sources of Endemic Human Coronaviruses. *Adv. Virus. Res.* **2018**, *100*, 163–188.
8. Zhou, P.; Yang, X.-L.; Wang, X.-G.; et al. A Pneumonia Outbreak Associated with a New Coronavirus of Probable Bat Origin. *Nature* **2020**, *579*, 270–273.

9. Spaan, W.; Cavanagh, D.; Horzinek, M. C. Coronaviruses: Structure and Genome Expression. *J. Gen. Virol*. **1988**, *69* (Pt. 12), 2939–2952.

10. Denison, M. R.; Graham, R. L.; Donaldson, E. F.; et al. Coronaviruses: An RNA Proofreading Machine Regulates Replication Fidelity and Diversity. *RNA Biol*. **2011**, *8*, 270–279.

11. Snijder, E. J.; Bredenbeek, P. J.; Dobbe, J. C.; et al. Unique and Conserved Features of Genome and Proteome of SARS-Coronavirus, an Early Split-Off from the Coronavirus Group 2 Lineage. *J. Mol. Biol*. **2003**, *331*, 991–1004.

12. Wu, F.; Zhao, S.; Yu, B.; et al. A New Coronavirus Associated with Human Respiratory Disease in China. *Nature* **2020**, *579*, 265–269.

13. Sola, I.; Almazan, F.; Zuniga, S.; et al. Continuous and Discontinuous RNA Synthesis in Coronaviruses. *Annu. Rev. Virol*. **2015**, *2*, 265–288.

14. Romano, M.; Ruggiero, A.; Squeglia, F.; et al. A Structural View of SARS-CoV-2 RNA Replication Machinery: RNA Synthesis, Proofreading and Final Capping. *Cells* **2020**, *9*, 1267.

15. Decroly, E.; Ferron, F.; Lescar, J.; et al. Conventional and Unconventional Mechanisms for Capping Viral mRNA. *Nat. Rev. Microbiol*. **2011**, *10*, 51–65.

16. Ferron, F.; Decroly, E.; Selisko, B.; et al. The Viral RNA Capping Machinery as a Target for Antiviral Drugs. *Antiviral Res*. **2012**, *96*, 21–31.

17. Decroly, E.; Debarnot, C.; Ferron, F.; et al. Crystal Structure and Functional Analysis of the SARS-Coronavirus RNA Cap 2′-O-Methyltransferase nsp10/nsp16 Complex. *PLoS Pathog*. **2011**, *7*, e1002059.

18. Bouvet, M.; Lugari, A.; Posthuma, C. C.; et al. Coronavirus Nsp10, a Critical Co-Factor for Activation of Multiple Replicative Enzymes. *J. Biol. Chem*. **2014**, *289*, 25783–25796.

19. Ivanov, K. A.; Thiel, V.; Dobbe, J. C.; et al. Multiple Enzymatic Activities Associated with Severe Acute Respiratory Syndrome Coronavirus Helicase. *J. Virol*. **2004**, *78*, 5619–5632.

20. Chen, Y.; Cai, H.; Pan, J.; et al. Functional Screen Reveals SARS Coronavirus Nonstructural Protein nsp14 as a Novel Cap N7 Methyltransferase. *Proc. Natl. Acad. Sci. U.S.A*. **2009**, *106*, 3484–3489.

21. Chen, Y.; Su, C.; Ke, M.; et al. Biochemical and Structural Insights into the Mechanisms of SARS Coronavirus RNA Ribose 2′-O-Methylation by nsp16/nsp10 Protein Complex. *PLoS Pathog*. **2011**, *7*, e1002294.

22. Bouvet, M.; Debarnot, C.; Imbert, I.; et al. In Vitro Reconstitution of SARS-Coronavirus mRNA Cap Methylation. *PLoS Pathog*. **2010**, *6*, e1000863.

23. Chen, Y.; Tao, J.; Sun, Y.; et al. Structure-Function Analysis of Severe Acute Respiratory Syndrome Coronavirus RNA Cap Guanine-N7-Methyltransferase. *J. Virol*. **2013**, *87*, 6296–6305.

24. Decroly, E.; Imbert, I.; Coutard, B.; et al. Coronavirus Nonstructural Protein 16 Is a Cap-0 Binding Enzyme Possessing (Nucleoside-2′O)-Methyltransferase Activity. *J. Virol*. **2008**, *82*, 8071–8084.

25. Aouadi, W.; Blanjoie, A.; Vasseur, J. J.; et al. Binding of the Methyl Donor *S*-Adenosyl-l-Methionine to Middle East Respiratory Syndrome Coronavirus 2′-O-Methyltransferase nsp16 Promotes Recruitment of the Allosteric Activator nsp10. *J. Virol*. **2017**, *91*, e02217-16.

26. Lugari, A.; Betzi, S.; Decroly, E.; et al. Molecular Mapping of the RNA Cap 2′-O-Methyltransferase Activation Interface between Severe Acute Respiratory Syndrome Coronavirus nsp10 and nsp16. *J. Biol. Chem*. **2010**, *285*, 33230–33241.

27. Rosas-Lemus, M.; Minasov, G.; Shuvalova, L.; et al. High-Resolution Structures of the SARS-CoV-2 2′-O-Methyl transferase Reveal Strategies for Structure-Based Inhibitor Design. *Sci. Signal*. **2020**, *13*, eabe1202.

28. Krafcikova, P.; Silhan, J.; Nencka, R.; et al. Structural Analysis of the SARS-CoV-2 Methyltransferase Complex Involved in RNA Cap Creation Bound to Sinefungin. *Nat. Commun*. **2020**, *11*, 3717.

29. Blazer, L. L.; Li, F.; Kennedy, S.; et al. A Suite of Biochemical Assays for Screening RNA Methyltransferase BCDIN3D. *SLAS Discov*. **2017**, *22*, 32–39.

30. McGovern, S. L.; Helfand, B. T.; Feng, B.; et al. A Specific Mechanism of Nonspecific Inhibition. *J. Med. Chem*. **2003**, *46*, 4265–4272.

31. Auld, D. S.; Inglese, J.; Dahlin, J. L. Assay Interference by Aggregation. In *Assay Guidance Manual*; Markossian, S., Sittampalam, G. S., Grossman, A., et al., Eds.; Eli Lilly & Company and the National Center for Advancing Translational Sciences: Bethesda, MD, **2004**.

32. Scheer, S.; Ackloo, S.; Medina, T. S.; et al. A Chemical Biology Toolbox to Study Protein Methyltransferases and Epigenetic Signaling. *Nat. Commun*. **2019**, *10*, 19.

33. Ferreira de Freitas, R.; Ivanochko, D.; Schapira, M. Methyltransferase Inhibitors: Competing with, or Exploiting the Bound Cofactor. *Molecules* **2019**, *24*, 4492.

34. Tse, L. V.; Meganck, R. M.; Graham, R. L.; et al. The Current and Future State of Vaccines, Antivirals and Gene Therapies against Emerging Coronaviruses. *Front. Microbiol*. **2020**, *11*, 658.